Application of New Fast Multipole Boundary Integral Equation Method to Elastostatic Crack Problems in Three Dimensions

Ken-ichi YOSHIDA*, Naoshi NISHIMURA** and Shoichi KOBAYASHI***

*Member of JSCE, M. Eng., Dept. of Global Env. Eng., Kyoto University(Kyoto 6068501 Japan)
**Member of JSCE, Dr. Eng., Assoc. Prof., Dept. of Global Env. Eng., Kyoto University(Kyoto 6068501 Japan)
***Member of JSCE, Dr. Eng., Prof., Dept. of Construction Eng., Fukui University of Technology(Fukui 9108505 Japan)

Fast Multipole Method (FMM) has been developed as a technique to reduce the computational cost and memory requirements in solving large scale problems. This paper discusses an application of the new FMM to three-dimensional boundary integral equation method (BIEM) for elastostatic crack problems. The boundary integral equation is discretised with collocation method. The resulting algebraic equation is solved with Generalised Minimum RESidual method (GMRES). The numerical results show that the new FMM is more efficient than the original FMM.

Key Words : *FMM, the new FMM, Crack, BIEM, GMRES*

1. Introduction

In spite of the advantage of reduction of dimensionality BIEM has been applied to relatively small problems so far, because the resulting matrix is dense. Indeed, this property leads to a serious exhaustion of the memory of a computer, since the memory requirement of BIEM is $O(N^2)$, where N is the number of unknowns. When one attempts to solve matrix equations with direct methods such as Crout's method, Gaussian elimination, etc. the required computational cost increases to $O(N^3)$. But the appearance of FMM changed the circumstances drastically. FMM reduces the computational cost to $O(N^{1+\alpha}(\log N)^{\beta})$ and the memory requirements to $O(N)$, where α and β are nonnegative numbers. With the help of FMM, BIEM can be applied to large scale problems.

FMM was initially investigated by Rokhlin[1] as a fast solver for integral equations for the two-dimensional Laplace equation, and then was applied to multibody problems with Coulombic potential by Greengard[2]. Since then FMM has been developed as a fast solution method for large scale problems. An application of FMM to BIEM has been investigated by several authors: e.g., by Nishimura et al.[3] for crack problems for the three-dimensional Laplace equation, by Fu et al.[4], Fukui et al.[5] and Takahashi et al.[6] for ordinary problems for three-dimensional elastostatics, by Yoshida et al.[7),8] for crack problems in three-dimensional elastostatics and by Fujiwara[9] and by Yoshida et al.[10] for three-dimensional elastodynamics.

In FMM the computational cost for the M2L translation dominates the performance especially in three-dimensional problems or problems dealing with the Helmholtz equation. In view of this Rokhlin introduced the diagonal form[11),12] so as to reduce the computational cost for the M2L translation. Recently the number of researches using diagonal forms is increasing. The use of the diagonal form has been investigated by several authors: Koc and Chew[13], Epton and Dembart[14], for example. However, the diagonal form proposed by Rokhlin is known to have numerical instabilities in dealing with the Laplace equation[15] or low frequency problems for the Helmholtz equation[16]. In order to overcome these problems Hrycak and Rokhlin[17] proposed a new FMM for the two-dimensional Laplace equation, Greengard and Rokhlin[18] and Cheng et al.[19] for the three-dimensional Laplace equation, and Greengard et al.[20] for the three-dimensional Helmholtz equation. Nishimura et al.[21] applied the new FMM to crack problems for the two-dimensional Laplace equation. An application of the new FMM to three-dimensional elastostatics is mentioned in Fu et al.[22] but they present only an integral representation for the fundamental solution of anisotropic elastostatics without FMM formulation or numerical examples. In this paper we discuss an application of the new FMM to three dimensional elastostatic crack problems. The results show that the new FMM is more efficient than the original FMM.

2. Formulation for integral equation

Let $S \subset R^3$, or a 'crack', be a union of smooth non-self-intersecting curved surfaces having smooth edges ∂S. Also let $\boldsymbol{n}$ be the unit normal vector to S. Our problem is to find a solution $\boldsymbol{u}$ of the equation of elastostatics

$$C_{ijkl}u_{k,lj} = 0 \quad \text{in } R^3 \setminus \overline{S}$$

subject to the boundary condition

$$t_i^{\pm} := C_{ijkl}u_{k,l}^{\pm}n_j = 0 \quad \text{on } S \tag{1}$$

regularity

$$\boldsymbol{\phi}(\boldsymbol{x}) := \boldsymbol{u}^+(\boldsymbol{x}) - \boldsymbol{u}^-(\boldsymbol{x}) = 0 \quad \text{on } \partial S \tag{2}$$

and an asymptotic condition given by

$$\boldsymbol{u}(\boldsymbol{x}) \to \boldsymbol{u}^{\infty}(\boldsymbol{x}) \quad \text{as} \quad |\boldsymbol{x}| \to \infty$$

where $\boldsymbol{u}$, C_{ijkl}, $\boldsymbol{t}$, $\boldsymbol{u}^{\infty}$ and $\boldsymbol{\phi}$ stand for the displacement, elasticity tensor, traction vector, a solution of the equation of elastostatics in the whole space and the crack opening displacement, respectively. Also, the superscript $+$ $(-)$ indicates the limit on S from the positive (negative) side of S where the positive side indicates the one into which the unit normal vector $\boldsymbol{n}$ points. The components of C_{ijkl} are expressed with Lamé's constants λ, μ and Kronecker's delta δ_{ij} as

$$C_{ijkl} = \lambda\delta_{ij}\delta_{kl} + \mu(\delta_{ik}\delta_{jl} + \delta_{il}\delta_{jk}).$$

The solution $\boldsymbol{u}$ to this problem has an integral representation given by

$$u_i(\boldsymbol{x}) = u_i^{\infty}(\boldsymbol{x}) + \int_S C_{cdjl}\frac{\partial}{\partial y_l}\Gamma_{ij}(\boldsymbol{x}-\boldsymbol{y})n_c(\boldsymbol{y})\phi_d(\boldsymbol{y})dS_y \qquad \boldsymbol{x} \in R^3 \setminus \overline{S} \tag{3}$$

where $\Gamma_{ij}(\boldsymbol{x}-\boldsymbol{y})$ is the fundamental solution of the equation of elastostatics expressed as

$$\Gamma_{ij}(\boldsymbol{x}-\boldsymbol{y}) = \frac{1}{8\pi\mu}\left(\delta_{ij}\frac{\partial}{\partial x_l}\frac{\partial}{\partial x_l} - \frac{\lambda+\mu}{\lambda+2\mu}\frac{\partial}{\partial x_i}\frac{\partial}{\partial x_j}\right)|\boldsymbol{x}-\boldsymbol{y}| \tag{4}$$

Using (1) and (3), one obtains the following hypersingular integral equation:

$$t_a^{\infty}(\boldsymbol{x}) = -\text{p.f.}\int_S n_b(\boldsymbol{x})C_{abik}\frac{\partial}{\partial x_k}\frac{\partial}{\partial y_l}\Gamma_{ij}(\boldsymbol{x}-\boldsymbol{y}) C_{cdjl}n_c(\boldsymbol{y})\phi_d(\boldsymbol{y})dS_y, \quad \boldsymbol{x} \in S \tag{5}$$

where $\boldsymbol{t}^{\infty}(\boldsymbol{x})$ and p.f. indicate the traction associated with $\boldsymbol{u}^{\infty}(\boldsymbol{x})$ and the finite part of a divergent integral.

Eq.(5) can also be written as

$$t_a^{\infty}(\boldsymbol{x}) = \text{v.p.}\int_S n_b(\boldsymbol{x})C_{abik}e_{rck}C_{cdjl}\frac{\partial}{\partial y_l}\Gamma_{ij}(\boldsymbol{x}-\boldsymbol{y}) e_{rqs}\frac{\partial\phi_d(\boldsymbol{y})}{\partial y_q}n_s(\boldsymbol{y})dS_y \tag{6}$$

where v.p. indicates Cauchy's principal value. In this paper we use (6) for the direct computation of (5).

3. Original FMM

In this section we present the formulation and algorithm for the original FMM to show differences between the original FMM and the new FMM.(See Yoshida et al.[7] for further details)

3.1 Formulation for original FMM

In the application of FMM to BIEM our starting point is to expand the fundamental solution $\Gamma_{ij}(\boldsymbol{x}-\boldsymbol{y})$ into a series of products of functions of $\boldsymbol{x}$ and those of $\boldsymbol{y}$. From the expression of (4) one finds that it is necessary to expand $|\boldsymbol{x}-\boldsymbol{y}|$ into a series. Yoshida et al.[7] obtained an expansion for $|\boldsymbol{x}-\boldsymbol{y}|$ as follows:

$$|\boldsymbol{x}-\boldsymbol{y}| = \sum_{n=0}^{\infty}\sum_{m=-n}^{n}\left(\frac{S_{n,m}(\overrightarrow{O\boldsymbol{x}})|\overrightarrow{O\boldsymbol{y}}|^2\overline{R_{n,m}}(\overrightarrow{O\boldsymbol{y}})}{2n+3} - \frac{|\overrightarrow{O\boldsymbol{x}}|^2S_{n,m}(\overrightarrow{O\boldsymbol{x}})\overline{R_{n,m}}(\overrightarrow{O\boldsymbol{y}})}{2n-1}\right) \quad (|\overrightarrow{O\boldsymbol{x}}| > |\overrightarrow{O\boldsymbol{y}}|) \tag{7}$$

where $R_{n,m}$ and $S_{n,m}$ are solid harmonic functions defined as

$$R_{n,m}(\overrightarrow{O\boldsymbol{x}}) = \frac{1}{(n+m)!}P_n^m(\cos\theta)e^{im\phi}r^n,$$

$$S_{n,m}(\overrightarrow{O\boldsymbol{x}}) = (n-m)!P_n^m(\cos\theta)e^{im\phi}\frac{1}{r^{n+1}},$$

(r, θ, ϕ) are the polar coordinates of the point $\boldsymbol{x}$, P_n^m is the associated Legendre function and a superposed bar indicates the complex conjugate. The use of solid harmonics in FMM has been suggested by Pérez-Jordá and Yang[24]. The functions $R_{n,m}$ and $S_{n,m}$ satisfy the following relations given by

$$S_{n,m}(\overrightarrow{\boldsymbol{y}\boldsymbol{x}}) = \sum_{n'=0}^{\infty}\sum_{m'=-n'}^{n'}\overline{R_{n',m'}}(\overrightarrow{O\boldsymbol{y}})S_{n+n',m+m'}(\overrightarrow{O\boldsymbol{x}}) \quad (|\overrightarrow{O\boldsymbol{y}}| < |\overrightarrow{O\boldsymbol{x}}|) \tag{8}$$

$$R_{n,m}(\overrightarrow{\boldsymbol{y}\boldsymbol{x}}) = \sum_{n'=0}^{n}\sum_{m'=-n'}^{n'}R_{n',m'}(\overrightarrow{\boldsymbol{y}O})R_{n-n',m-m'}(\overrightarrow{O\boldsymbol{x}}) \quad \text{(This holds for arbitrary } \overrightarrow{O\boldsymbol{x}} \text{ and } \overrightarrow{O\boldsymbol{y}}) \tag{9}$$

Using (7), one rewrites (4) as[7)]

$$\Gamma_{ij}(\boldsymbol{x}-\boldsymbol{y}) = \frac{1}{8\pi\mu}\sum_{n=0}^{\infty}\sum_{m=-n}^{n}\Big(F^S_{ij,n,m}(\overrightarrow{O\boldsymbol{x}})\overline{R_{n,m}}(\overrightarrow{O\boldsymbol{y}}) + G^S_{i,n,m}(\overrightarrow{O\boldsymbol{x}})(\overrightarrow{O\boldsymbol{y}})_j\overline{R_{n,m}}(\overrightarrow{O\boldsymbol{y}})\Big) \tag{10}$$

where $F^S_{ij,n,m}$ and $G^S_{i,n,m}$ are functions defined as[7)]

$$F^S_{ij,n,m}(\overrightarrow{O\boldsymbol{x}}) = \frac{\lambda+3\mu}{\lambda+2\mu}\delta_{ij}S_{n,m}(\overrightarrow{O\boldsymbol{x}}) - \frac{\lambda+\mu}{\lambda+2\mu}(\overrightarrow{O\boldsymbol{x}})_j\frac{\partial}{\partial x_i}S_{n,m}(\overrightarrow{O\boldsymbol{x}}) \tag{11}$$

$$G^S_{i,n,m}(\overrightarrow{O\boldsymbol{x}}) = \frac{\lambda+\mu}{\lambda+2\mu}\frac{\partial}{\partial x_i}S_{n,m}(\overrightarrow{O\boldsymbol{x}}) \tag{12}$$

We now compute the integral on the right hand side of (5) over a subset of S denoted by S_y for $\boldsymbol{x}$ which is away from S_y. Using (10) we obtain

$$-\text{p.f.}\int_{S_y}\frac{\partial}{\partial x_k}\frac{\partial}{\partial y_l}\Gamma_{ij}(\boldsymbol{x}-\boldsymbol{y})C_{cdjl}n_c(\boldsymbol{y})\phi_d(\boldsymbol{y})dS_y = -\frac{1}{8\pi\mu}\sum_{n=0}^{\infty}\sum_{m=-n}^{n}\Big(\frac{\partial}{\partial x_k}F^S_{ij,n,m}(\overrightarrow{O\boldsymbol{x}})\overline{M^1_{j,n,m}}(O) + \frac{\partial}{\partial x_k}G^S_{i,n,m}(\overrightarrow{O\boldsymbol{x}})\overline{M^2_{n,m}}(O)\Big) \tag{13}$$

where $M^1_{j,n,m}$ and $M^2_{n,m}$ are the multipole moments centred at O, expressed as

$$M^1_{j,n,m}(O) = \int_{S_y}C_{cdjl}\frac{\partial}{\partial y_l}R_{n,m}(\overrightarrow{O\boldsymbol{y}})\phi_d(\boldsymbol{y})n_c(\boldsymbol{y})dS_y, \tag{14}$$

$$M^2_{n,m}(O) = \int_{S_y}C_{cdjl}\frac{\partial}{\partial y_l}((\overrightarrow{O\boldsymbol{y}})_jR_{n,m}(\overrightarrow{O\boldsymbol{y}}))\phi_d(\boldsymbol{y})n_c(\boldsymbol{y})dS_y. \tag{15}$$

The multipole moments are translated according to the following formulae as the centre of multipole expansion is shifted from O to O':

$$M^1_{j,n,m}(O') = \sum_{n'=0}^{n}\sum_{m'=-n'}^{n'}R_{n',m'}(\overrightarrow{O'O})M^1_{j,n-n',m-m'}(O) \tag{16}$$

$$M^2_{n,m}(O') = \sum_{n'=0}^{n}\sum_{m'=-n'}^{n'}R_{n',m'}(\overrightarrow{O'O})\big(M^2_{n-n',m-m'}(O) - (\overrightarrow{OO'})_jM^1_{j,n-n',m-m'}(O)\big) \tag{17}$$

where we have used (9), (14) and (15). In the evaluation of the integral on the right hand side of (5) one can use not only the multipole moments but also the coefficients of local expansion in the following manner:

$$-\text{p.f.}\int_{S_y}\frac{\partial}{\partial x_k}\frac{\partial}{\partial y_l}\Gamma_{ij}(\boldsymbol{x}-\boldsymbol{y})C_{cdjl}n_c(\boldsymbol{y})\phi_d(\boldsymbol{y})dS_y = -\frac{1}{8\pi\mu}\sum_{n=0}^{\infty}\sum_{m=-n}^{n}\Big(\frac{\partial}{\partial x_k}F^R_{ij,n,m}(\overrightarrow{\boldsymbol{x}_0\boldsymbol{x}})L^1_{j,n,m}(\boldsymbol{x}_0) + \frac{\partial}{\partial x_k}G^R_{i,n,m}(\overrightarrow{\boldsymbol{x}_0\boldsymbol{x}})L^2_{n,m}(\boldsymbol{x}_0)\Big) \tag{18}$$

where $L^1_{j,n,m}$ and $L^2_{n,m}$ are expressed with $M^1_{j,n,m}$ and $M^2_{n,m}$ by

$$L^1_{j,n',m'}(\boldsymbol{x}_0) = \sum_{n=0}^{\infty}\sum_{m=-n}^{n}(-1)^{n'}\overline{S_{n+n',m+m'}}(\overrightarrow{O\boldsymbol{x}_0})M^1_{j,n,m}(O) \tag{19}$$

$$L^2_{n',m'}(\boldsymbol{x}_0) = \sum_{n=0}^{\infty}\sum_{m=-n}^{n}(-1)^{n'}\overline{S_{n+n',m+m'}}(\overrightarrow{O\boldsymbol{x}_0}) \times(M^2_{n,m}(O) - (\overrightarrow{O\boldsymbol{x}_0})_jM^1_{j,n,m}(O)) \tag{20}$$

and $F^R_{ij,n,m}$ and $G^R_{i,n,m}$ are functions obtained by replacing $S_{n,m}$ by $R_{n,m}$ in (11) and (12). In these formulae we have used (8) and have assumed that the inequality $|\overrightarrow{O\boldsymbol{x}_0}| > |\overrightarrow{\boldsymbol{x}_0\boldsymbol{x}}|$ holds. The procedures given by (19) and (20) are called M2L translation.

The coefficients of the local expansion are translated according to the following formulae when the centre of the local expansion is shifted from $\boldsymbol{x}_0$ to $\boldsymbol{x}_1$

$$L^1_{j,n'',m''}(\boldsymbol{x}_1) = \sum_{n'=n''}^{\infty}\sum_{m'=-n'}^{n'}R_{n'-n'',m'-m''}(\overrightarrow{\boldsymbol{x}_0\boldsymbol{x}_1})L^1_{j,n',m'}(\boldsymbol{x}_0) \tag{21}$$

$$L^2_{n'',m''}(\boldsymbol{x}_1) = \sum_{n'=n''}^{\infty}\sum_{m'=-n'}^{n'}R_{n'-n'',m'-m''}(\overrightarrow{\boldsymbol{x}_0\boldsymbol{x}_1}) \times\big(L^2_{n',m'}(\boldsymbol{x}_0) - (\overrightarrow{\boldsymbol{x}_0\boldsymbol{x}_1})_pL^1_{p,n',m'}(\boldsymbol{x}_0)\big) \tag{22}$$

where we have used (9) and (18).

3.2 Algorithm for original FMM

The algorithm of the original FMM is described as follows:

Step 1. Discretisation:
Discretise S in the same manner as in the conventional BIEM.

Step 2. Determination of octtree structure:
Consider a cube which circumscribes S and call this cube the cell of level 0. Now take a cell (a parent cell) of level l ($l \geq 0$) and divide it into 8 equal sub cubes whose edge length is half of that

of the parent cell and call any of them which contains some boundary elements a cell of level $l+1$. Continue the subdivision of cells until the number of boundary elements in the cell is below a given number. A cell having no children is called a leaf.

Step 3. Computation of the multipole moments: First compute the multipole moments associated with leaves via (14) and (15) taking the centre (O) of the multipole moment as the centroid of C. Now consider a non-leaf cell C of level l. We compute the multipole moments associated with C by translating the multipole moments of C's children via (16) and (17) with the origin shifted from the centroids of C's children (O) to that of C (O') and adding all the translated multipole moments of C's children. We repeat this procedure tracing the tree structure of cells upward (decreasing l) until we reach level 2 cells.

Step 4. Computation of the local expansion: We have to prepare some definitions first. We say that two cells are 'adjacent cells at level l' if these cells are both of the level l and share at least one vertex. Two cells are said to be 'well-separated at level l' if they are not adjacent at level l but their parent cells are adjacent at level $l-1$. The list of all the well-separated cells from a level l cell C is called the interaction list of C.

Now we compute the local expansion associated with a cell C. The local expansion associated with C represents a sum of the contribution due to boundary elements in cells of the interaction list of C and the contribution due to all boundary elements in cells which are not adjacent to C's parent. The former is computed by substituting the multipole moments associated with cells of the interaction list of C to (19) and (20) and the latter by translating the local expansion associated with C's parent via (21) and (22) as the centre of the local expansion is shifted from the centroid of C's parent ($\boldsymbol{x}_0$) to the centroid of C ($\boldsymbol{x}_1$). The sum of these contributions gives the local expansion associated with C. We repeat these procedures starting from $l=2$ and increasing l along the tree structure until we reach leaves. When $l=2$, the coefficients of the local expansion are computed only by using (19) and (20). This is because cells of level 1 have no well-separated cells.

Step 5. Evaluation of the integral in (5): We now compute the integral in (5) at leaves (denoted by C). First we compute the contribution from boundary elements in cells adjacent to C using (6) in the same manner as in the conventional BIEM and then compute the contribution from cells which are not adjacent to C using (18). The sum of these contributions describes the contribution from all boundary elements.

4. New FMM

In this section we present the formulation and algorithm for the new FMM.

4.1 Formulation for the new FMM

Now we consider a source point $\boldsymbol{y}$ located at (y_1, y_2, y_3) and a target point $\boldsymbol{x}$ at (x_1, x_2, x_3) and denote a cell including a source point by C_s and a cell including a target point by C_t. Here we introduce the following integral representation:

$$\frac{1}{\sqrt{(x_1-y_1)^2+(x_2-y_2)^2+(x_3-y_3)^2}} = \frac{1}{2\pi}\int_0^\infty e^{-\lambda(x_3-y_3)} \int_0^{2\pi} e^{i\lambda((x_1-y_1)\cos\alpha+(x_2-y_2)\sin\alpha)}d\alpha d\lambda \quad (23)$$

The integral in (23) converges under an assumption that the inequality $x_3 > y_3$ is valid. This is why we restrict the discussion to the case where C_t is located in $+x_3$ direction of C_s for the present. Suppose that each of the cells C_s and C_t has a volume of d^3. Then the double integral in (23) is evaluated with the following double sum:

$$\frac{1}{\sqrt{(x_1-y_1)^2+(x_2-y_2)^2+(x_3-y_3)^2}} = \sum_{k=1}^{s(\varepsilon)}\sum_{j=1}^{M(k)} \frac{\omega_k}{M(k)d} e^{-(\lambda_k/d)(x_3-y_3)} e^{i(\lambda_k/d)((x_1-y_1)\cos\alpha_j(k)+(x_2-y_2)\sin\alpha_j(k))} + \varepsilon, \quad (x_3 > y_3) \quad (24)$$

where $\alpha_j(k)$ is given by

$$\alpha_j(k) = \frac{2\pi j}{M(k)},$$

ε is the error term and the numbers $s(\varepsilon)$, $M(k)$, Gaussian weights ω_k and nodes λ_k are given in Yarvin and Rokhlin[23]. One may determine these parameters considering the required accuracy.

Noting the following formulae:

$$S_{n,m}(\overrightarrow{O\boldsymbol{x}}) = (-1)^n \partial_+^m \partial_z^{n-m}\left(\frac{1}{r}\right) \quad (m \geq 0),$$

$$S_{n,-m}(\overrightarrow{O\boldsymbol{x}}) = (-1)^{n+m} \partial_-^m \partial_z^{n-m}\left(\frac{1}{r}\right) \quad (m \geq 0),$$

$$\partial_\pm = \left(\frac{\partial}{\partial x} \pm i\frac{\partial}{\partial y}\right)$$

and (24), one can evaluate the integral in (5) in the following manner:

$$\text{p.f.}\int_{S_y} \frac{\partial}{\partial x_k}\frac{\partial}{\partial y_l}\Gamma_{ij}(\boldsymbol{x}-\boldsymbol{y})C_{cdjl}n_c(\boldsymbol{y})\phi_d(\boldsymbol{y})dS_y$$

$$= \frac{1}{8\pi} \sum_{p=1}^{s(\varepsilon)} \sum_{q=1}^{M(p)} \left(\mathcal{F}_{kij}(\overrightarrow{Ox}) W_j^1(p,q) + \mathcal{G}_{ki}(\overrightarrow{Ox}) W^2(p,q) \right)$$
$$e^{-(\lambda_p/d)(\overrightarrow{Ox})_3 + i(\lambda_p/d)((\overrightarrow{Ox})_1 \cos\alpha_q(p) + (\overrightarrow{Ox})_2 \sin\alpha_q(p))}$$

where $W_j^1(p,q)$ and $W^2(p,q)$ are the coefficients of the exponential expansion at O, defined as

$$W_j^1(p,q) = \frac{\omega_p}{M(p)d} \sum_{m=-\infty}^{\infty} (-i)^m e^{-im\alpha_q(p)} \sum_{n=|m|}^{\infty} (\lambda_p/d)^n M_{j,n,m}^1(O) \tag{25}$$

$$W^2(p,q) = \frac{\omega_p}{M(p)d} \sum_{m=-\infty}^{\infty} (-i)^m e^{-im\alpha_q(p)} \sum_{n=|m|}^{\infty} (\lambda_p/d)^n M_{n,m}^2(O) \tag{26}$$

and $\mathcal{F}, \mathcal{G}$ are operators defined as

$$\mathcal{F}_{kij}(\overrightarrow{Ox}) = \frac{\lambda+3\mu}{\lambda+2\mu} \frac{\partial}{\partial x_k} \delta_{ij} - \frac{\lambda+\mu}{\lambda+2\mu} \frac{\partial}{\partial x_k} (\overrightarrow{Ox})_j \frac{\partial}{\partial x_i}$$
$$\mathcal{G}_{ki}(\overrightarrow{Ox}) = \frac{\lambda+\mu}{\lambda+2\mu} \frac{\partial}{\partial x_k} \frac{\partial}{\partial x_i}$$

These formulae (25) and (26) convert the multipole moments into the coefficients of the exponential expansion. The coefficients of the exponential expansion is translated according to the following formulae when the centre of the exponential expansion is shifted from O to $\boldsymbol{x}_0$:

$$V_j^1(p,q) = W_j^1(p,q)$$
$$e^{-(\lambda_p/d)(\overrightarrow{Ox_0})_3 + i(\lambda_p/d)((\overrightarrow{Ox_0})_1 \cos\alpha_q(p) + (\overrightarrow{Ox_0})_2 \sin\alpha_q(p))} \tag{27}$$

$$V^2(p,q) = (W^2(p,q) - (\overrightarrow{Ox_0})_k W_k^1(p,q))$$
$$e^{-(\lambda_p/d)(\overrightarrow{Ox_0})_3 + i(\lambda_p/d)((\overrightarrow{Ox_0})_1 \cos\alpha_q(p) + (\overrightarrow{Ox_0})_2 \sin\alpha_q(p))} \tag{28}$$

where $V_j^1(p,q)$ and $V^2(p,q)$ are the coefficients of the exponential expansion at $\boldsymbol{x}_0$ and $(\boldsymbol{x})_i$ stand for the components of the vector $\boldsymbol{x}$.

We next need to convert the coefficients of the exponential expansion into the coefficients of the local expansion. Noting that the integral in (13) is evaluated with $V_j^1(p,q)$ and $V^2(p,q)$ as follows:

$$\text{p.f.} \int_{S_y} \frac{\partial}{\partial x_k} \frac{\partial}{\partial y_l} \Gamma_{ij}(\boldsymbol{x}-\boldsymbol{y}) C_{cdjl} n_c(\boldsymbol{y}) \phi_d(\boldsymbol{y}) dS_y$$
$$= \frac{1}{8\pi} \sum_{p=1}^{s(\varepsilon)} \sum_{q=1}^{M(p)} \left(\mathcal{F}_{kij}(\overrightarrow{x_0 x}) V_j^1(p,q) + \mathcal{G}_{ki}(\overrightarrow{x_0 x}) V^2(p,q) \right)$$
$$e^{-(\lambda_p/d)(\overrightarrow{x_0 x})_3 + i(\lambda_p/d)((\overrightarrow{x_0 x})_1 \cos\alpha_q(p) + (\overrightarrow{x_0 x})_2 \sin\alpha_q(p))}$$

and using (18) and the following formula:

$$\sum_{m=-n}^{n} (-i)^m e^{-im\alpha_j(k)} R_{n,m}(\overrightarrow{Ox}) =$$
$$\frac{((\overrightarrow{Ox})_3 - i(\overrightarrow{Ox})_1 \cos\alpha_j(k) - i(\overrightarrow{Ox})_2 \sin\alpha_j(k))^n}{n!}$$

one obtains the following formulae which converts the coefficients of the exponential expansion into the coefficient of the local expansion:

$$L_{j,n,m}^1(\boldsymbol{x}_0) = \sum_{p=1}^{s(\varepsilon)} \sum_{q=1}^{M(p)} V_j^1(p,q) (-i)^m (-\lambda_p/d)^n e^{-im\alpha_q(p)} \tag{29}$$

$$L_{n,m}^2(\boldsymbol{x}_0) = \sum_{p=1}^{s(\varepsilon)} \sum_{q=1}^{M(p)} V^2(p,q) (-i)^m (-\lambda_p/d)^n e^{-im\alpha_q(p)} \tag{30}$$

The procedures in (25)–(30) correspond to the M2L translation expressed by (19) and (20) for the original FMM. Suppose that one truncates the infinite series in (10) taking p terms. Then the computational costs for (19) and (20) are obviously $O(p^4)$. Also, if one assumes

$$\sum_{k=1}^{s(\varepsilon)} M(k) \approx p^2, \quad s(\varepsilon) \approx p,$$

the computational costs for (25) and (26), (27) and (28) and (29) and (30) are $O(p^3)$, $O(p^2)$ and $O(p^3)$, respectively. Hence, the total cost for the procedures in (25)–(30) is $O(p^3)$. This is why the new FMM is faster than the original FMM.

4.2 Rotation of coefficients

The discussion in the previous section has been restricted to the case where C_t is in $+x_3$ direction of C_s. In this section we shall remove this assumption to generalise the discussion. We divide the interaction list of C_s into 6 lists: uplist, downlist, northlist, southlist, eastlist and westlist. The uplist and downlist contain target cells located in $+x_3$ and $-x_3$ directions of C_s, respectively. The northlist and southlist contain target cells located in $+x_2$ and $-x_2$ directions of C_s except those in the uplist or downlist, respectively. The eastlist and westlist contain target cells located in $+x_1$ and $-x_1$ directions of C_s except those in the uplist, downlist, northlist or southlist, respectively. The situation in the previous section can be described as the case where C_t is contained in the uplist of C_s. If the target cell is included in lists except the uplist of C_s we rotate the coordinate system so that the target cell is in the positive $\tilde{x}_3$ direction viewed from the source cell, where $\tilde{x}_i$ denotes the new axis. In general the multipole moments in the new coordinate system are obtained as follows:

$$\widetilde{M}_{j,n,m}^1(O) = \mathcal{A}_{ji} \sum_{m'=-n}^{n} \mathcal{R}_{n,m,m'}(\boldsymbol{\nu}, \alpha) M_{i,n,m'}^1(O)$$

(31)

$$\widetilde{M}^2_{n,m}(O) = \sum_{m'=-n}^{n} \mathcal{R}_{n,m,m'}(\boldsymbol{\nu}, \alpha) M^2_{n,m'}(O)$$

(32)

where $\mathcal{R}_{n,m,m'}(\boldsymbol{\nu}, \alpha)$ is the coefficient of rotation, $\boldsymbol{\nu}$ is a unit vector parallel to the rotation axis, α is a rotation angle and $\mathcal{A}_{ij}$ is a rotation matrix. The explicit form of $\mathcal{R}_{n,m,m'}(\boldsymbol{\nu}, \alpha)$ is given by (See Biedenharn and Louck[25])

$$\begin{aligned}
&\mathcal{R}_{n,m,m'}(\boldsymbol{\nu}, \alpha) = (-1)^{m+m'}(n+m')!(n-m')! \\
&\sum_k \Big[(\alpha_0 - i\alpha_3)^{n+m-k}(-i\alpha_1 - \alpha_2)^{m'-m+k} \\
&(-i\alpha_1 + \alpha_2)^k(\alpha_0 + i\alpha_3)^{n-m'-k}\Big] [(n+m-k)! \\
&(m'-m+k)!k!(n-m'-k)!]^{-1}
\end{aligned} \tag{33}$$

where $\alpha_0 = \cos(\alpha/2)$ and $\alpha_i = -\nu_i \sin(\alpha/2)$. The summation in (33) is carried out over such k that the powers in the numerator are all non-negative.

We next describe the generalised M2L translation process in the new FMM.

1. Rotation:
   First we rotate the multipole moments via (31) and (32) so as to make the procedure presented in 4.1 applicable. The specific forms of (31) and (32) depend on the location of C_t and are described as follows:
   - $C_t \in$ uplist

$$\widetilde{M}^{1U}_{j,n,m}(O) = \mathcal{A}^U_{ji} M^1_{i,n,m}(O) \tag{34}$$

$$\widetilde{M}^{2U}_{n,m}(O) = M^2_{n,m}(O) \tag{35}$$

   - $C_t \in$ downlist

$$\widetilde{M}^{1D}_{j,n,m}(O) = \mathcal{A}^D_{ji} \sum_{m'=-n}^{n} \mathcal{R}_{n,m,m'}(\boldsymbol{e}_1, \pi) M^1_{i,n,m'}(O) \tag{36}$$

$$\widetilde{M}^{2D}_{n,m}(O) = \sum_{m'=-n}^{n} \mathcal{R}_{n,m,m'}(\boldsymbol{e}_1, \pi) M^2_{n,m'}(O) \tag{37}$$

   - $C_t \in$ northlist

$$\widetilde{M}^{1N}_{j,n,m}(O) = \mathcal{A}^N_{ji} \sum_{m'=-n}^{n} \mathcal{R}_{n,m,m'}(\boldsymbol{e}_1, \pi/2) M^1_{i,n,m'}(O) \tag{38}$$

$$\widetilde{M}^{2N}_{n,m}(O) = \sum_{m'=-n}^{n} \mathcal{R}_{n,m,m'}(\boldsymbol{e}_1, \pi/2) M^2_{n,m'}(O) \tag{39}$$

   - $C_t \in$ southlist

$$\widetilde{M}^{1S}_{j,n,m}(O) = \mathcal{A}^S_{ji} \sum_{m'=-n}^{n} \mathcal{R}_{n,m,m'}(\boldsymbol{e}_1, -\pi/2) M^1_{i,n,m'}(O) \tag{40}$$

$$\widetilde{M}^{2S}_{n,m}(O) = \sum_{m'=-n}^{n} \mathcal{R}_{n,m,m'}(\boldsymbol{e}_1, -\pi/2) M^2_{n,m'}(O) \tag{41}$$

   - $C_t \in$ eastlist

$$\widetilde{M}^{1E}_{j,n,m}(O) = \mathcal{A}^E_{ji} \sum_{m'=-n}^{n} \mathcal{R}_{n,m,m'}(\boldsymbol{e}_2, -\pi/2) M^1_{i,n,m'}(O) \tag{42}$$

$$\widetilde{M}^{2E}_{n,m}(O) = \sum_{m'=-n}^{n} \mathcal{R}_{n,m,m'}(\boldsymbol{e}_2, -\pi/2) M^2_{n,m'}(O) \tag{43}$$

   - $C_t \in$ westlist

$$\widetilde{M}^{1W}_{j,n,m}(O) = \mathcal{A}^W_{ji} \sum_{m'=-n}^{n} \mathcal{R}_{n,m,m'}(\boldsymbol{e}_2, \pi/2) M^1_{i,n,m'}(O) \tag{44}$$

$$\widetilde{M}^{2W}_{n,m}(O) = \sum_{m'=-n}^{n} \mathcal{R}_{n,m,m'}(\boldsymbol{e}_2, \pi/2) M^2_{n,m'}(O) \tag{45}$$

   where $\boldsymbol{e}_i$ is the base vector for the Cartesian coordinates and superposed indices $\{U, D, N, S, E, W\}$ correspond to the initial letters of {uplist, downlist, northlist, southlist, eastlist, westlist}, respectively.
2. Compute the coefficients of the exponential expansion:
   Compute the coefficients of the exponential expansion via (25) and (26) as follows:

$$W^{1\Diamond}_j(p,q) = \frac{\omega_p}{M(p)d} \sum_{m=-\infty}^{\infty} (-i)^m e^{-im\alpha_q(p)} \sum_{n=|m|}^{\infty} (\lambda_p/d)^n \widetilde{M}^{1\Diamond}_{j,n,m}(O) \tag{46}$$

$$W^{2\Diamond}(p,q) = \frac{\omega_p}{M(p)d} \sum_{m=-\infty}^{\infty} (-i)^m e^{-im\alpha_q(p)} \sum_{n=|m|}^{\infty} (\lambda_p/d)^n \widetilde{M}^{2\Diamond}_{n,m}(O) \tag{47}$$

where $\diamondsuit$ is an element of $\{U, D, N, S, E, W\}$.

3. Translation of the coefficients of the exponential expansion:
   As the centre of the exponential expansion is shifted from the centroid of C_s (O) to the centroid of C_t $(\boldsymbol{x}_0)$, the coefficients of the exponential expansion is translated according to (27) and (28) as follows:

$$V_j^{1\diamondsuit}(p,q) = W_j^{1\diamondsuit}(p,q) \\ e^{-(\lambda_p/d)(\widetilde{O\boldsymbol{x}_0})_3 + i(\lambda_p/d)((\widetilde{O\boldsymbol{x}_0})_1 \cos\alpha_q(p) + (\widetilde{O\boldsymbol{x}_0})_2 \sin\alpha_q(p))} \tag{48}$$

$$V^{2\diamondsuit}(p,q) = (W^{2\diamondsuit}(p,q) - W_k^{1\diamondsuit}(p,q)(\widetilde{O\boldsymbol{x}_0})_k) \\ e^{-(\lambda_p/d)(\widetilde{O\boldsymbol{x}_0})_3 + i(\lambda_p/d)((\widetilde{O\boldsymbol{x}_0})_1 \cos\alpha_q(p) + (\widetilde{O\boldsymbol{x}_0})_2 \sin\alpha_q(p))} \tag{49}$$

$$(\widetilde{O\boldsymbol{x}_0})_i = A_{ij}^{\diamondsuit}(\overrightarrow{O\boldsymbol{x}_0})_j$$

   where $\diamondsuit$ is an element of $\{U, D, N, S, E, W\}$.

4. Compute the coefficients of the local expansion:
   Compute the coefficients of the local expansion from the exponential expansion according to (29) and (30) as follows:

$$\widetilde{L}_{j,n,m}^{1\diamondsuit}(\boldsymbol{x}_0) = \\ \sum_{p=1}^{s(\varepsilon)} \sum_{q=1}^{M(p)} V_j^{1\diamondsuit}(p,q)(-i)^m(-\lambda_p/d)^n e^{-im\alpha_q(p)} \tag{50}$$

$$\widetilde{L}_{n,m}^{2\diamondsuit}(\boldsymbol{x}_0) = \\ \sum_{p=1}^{s(\varepsilon)} \sum_{q=1}^{M(p)} V^{2\diamondsuit}(p,q)(-i)^m(-\lambda_p/d)^n e^{-im\alpha_q(p)} \tag{51}$$

   where $\diamondsuit$ is an element of $\{U, D, N, S, E, W\}$. Then rotate $\tilde{L}_{n,m}^{\diamondsuit}$ as follows:

   - $C_t \in$ uplist

$$L_{j,n,m}^{1U}(\boldsymbol{x}_0) = \mathcal{A}_{ij}^{U} \widetilde{L}_{i,n,m}^{1U}(\boldsymbol{x}_0) \tag{52}$$

$$L_{n,m}^{2U}(\boldsymbol{x}_0) = \widetilde{L}_{n,m}^{2U}(\boldsymbol{x}_0) \tag{53}$$

   - $C_t \in$ downlist

$$L_{j,n,m}^{1D}(\boldsymbol{x}_0) = \\ \mathcal{A}_{ij}^{D} \sum_{m'=-n}^{n} \mathcal{R}_{n,m',m}(\boldsymbol{e}_1, \pi) \widetilde{L}_{i,n,m'}^{1D}(\boldsymbol{x}_0) \tag{54}$$

$$L_{n,m}^{2D}(\boldsymbol{x}_0) = \\ \sum_{m'=-n}^{n} \mathcal{R}_{n,m',m}(\boldsymbol{e}_1, \pi) \widetilde{L}_{n,m'}^{2D}(\boldsymbol{x}_0) \tag{55}$$

   - $C_t \in$ northlist

$$L_{j,n,m}^{1N}(\boldsymbol{x}_0) = \\ \mathcal{A}_{ij}^{N} \sum_{m'=-n}^{n} \mathcal{R}_{n,m',m}(\boldsymbol{e}_1, \pi/2) \widetilde{L}_{i,n,m'}^{1N}(\boldsymbol{x}_0) \tag{56}$$

$$L_{n,m}^{2N}(\boldsymbol{x}_0) = \\ \sum_{m'=-n}^{n} \mathcal{R}_{n,m',m}(\boldsymbol{e}_1, \pi/2) \widetilde{L}_{n,m'}^{2N}(\boldsymbol{x}_0) \tag{57}$$

   - $C_t \in$ southlist

$$L_{j,n,m}^{1S}(\boldsymbol{x}_0) = \\ \mathcal{A}_{ij}^{S} \sum_{m'=-n}^{n} \mathcal{R}_{n,m',m}(\boldsymbol{e}_1, -\pi/2) \widetilde{L}_{i,n,m'}^{1S}(\boldsymbol{x}_0) \tag{58}$$

$$L_{n,m}^{2S}(\boldsymbol{x}_0) = \\ \sum_{m'=-n}^{n} \mathcal{R}_{n,m',m}(\boldsymbol{e}_1, -\pi/2) \widetilde{L}_{n,m'}^{2S}(\boldsymbol{x}_0) \tag{59}$$

   - $C_t \in$ eastlist

$$L_{j,n,m}^{1E}(\boldsymbol{x}_0) = \\ \mathcal{A}_{ij}^{E} \sum_{m'=-n}^{n} \mathcal{R}_{n,m',m}(\boldsymbol{e}_2, -\pi/2) \widetilde{L}_{i,n,m'}^{1E}(\boldsymbol{x}_0) \tag{60}$$

$$L_{n,m}^{2E}(\boldsymbol{x}_0) = \\ \sum_{m'=-n}^{n} \mathcal{R}_{n,m',m}(\boldsymbol{e}_2, -\pi/2) \widetilde{L}_{n,m'}^{2E}(\boldsymbol{x}_0) \tag{61}$$

   - $C_t \in$ westlist

$$L_{j,n,m}^{1W}(\boldsymbol{x}_0) = \\ \mathcal{A}_{ij}^{W} \sum_{m'=-n}^{n} \mathcal{R}_{n,m',m}(\boldsymbol{e}_2, \pi/2) \widetilde{L}_{i,n,m'}^{1W}(\boldsymbol{x}_0) \tag{62}$$

$$L_{n,m}^{2W}(\boldsymbol{x}_0) = \\ \sum_{m'=-n}^{n} \mathcal{R}_{n,m',m}(\boldsymbol{e}_2, \pi/2) \widetilde{L}_{n,m'}^{2W}(\boldsymbol{x}_0) \tag{63}$$

   Finally add L^U, L^D, L^N, L^S, L^E and L^W together

$$L_{j,n,m}^{1}(\boldsymbol{x}_0) = \sum_{\diamondsuit \in U,D,N,S,E,W} L_{j,n,m}^{1\diamondsuit}(\boldsymbol{x}_0) \tag{64}$$

$$L_{n,m}^{2}(\boldsymbol{x}_0) = \sum_{\diamondsuit \in U,D,N,S,E,W} L_{n,m}^{2\diamondsuit}(\boldsymbol{x}_0) \tag{65}$$

   to obtain the coefficients of the local expansion.

4.3 Algorithm for the new FMM

The algorithm for the new FMM is given as follows:

Steps 1–3. Same as the steps 1–3 in 3.2.

Step 4. Computation of the coefficients of the exponential expansion:

Compute the coefficients of the exponential expansion at each cell using (34)–(47), taking the origin (O) at the centroid of the cell.

Step 5. Computation of the coefficients of the local expansion:

We compute the coefficients of the local expansion of cells of level l, starting from $l = 2$ and increasing l. Now we consider cell C and cell C' which is contained in the interaction list of C. Considering the position of C' relative to C, we translate the coefficients of the exponential expansion via (48) and (49) as the centre of the exponential expansion is shifted from the centroid of C (O) to that of C' ($\boldsymbol{x}_0$) and then use appropriate formulae in (50)–(63) to convert the coefficients of the exponential expansion to the coefficients of the local expansion. After carrying out these conversions about all cells in the interaction list of C, we add them together via (64) and (65) to obtain the contribution from the interaction list of C to the coefficients of the local expansion. To these contributions we add the coefficients of the local expansion of the parent of C with the origin shifted from the centroid of the parent ($\boldsymbol{x}_0$) to that of C ($\boldsymbol{x}_1$) via (21) and (22) to obtain the coefficients of the local expansion associated with C.

Step 6. Same as the 5th step in 3.2.

5. Numerical Examples

The proposed techniques have been implemented in Fortran 77 and have been tested on a computer having a DEC Alpha 21264(500 MHz) as the CPU. The integrals in the multipole moments in (14) and (15) are computed numerically with Gaussian quadrature. The sums in the finite series (13) and (18) are truncated at 10 terms and the series in (46), (47), (50) and (51) are computed with the 109 point generalised Gaussian quadrature formula in Yarvin and Rokhlin[23]. The maximum number of boundary elements in a leaf is set to be 100. To solve the resulting matrix equation we use the preconditioned GMRES and adopt the block diagonal matrix corresponding to the leaves as the preconditioner according to Nishida and Hayami[26]. In GMRES the iteration is stopped when the relative residual norm is below 10^{-5}.

5.1 One crack

In the beginning we consider an infinite space which contains a penny-shaped crack having the radius of a_0 and the unit normal vector of $\boldsymbol{n} = (0, 0, 1)$. The function $\boldsymbol{t}^{\infty}(\boldsymbol{x})$ is given by $\boldsymbol{t}^{\infty}(\boldsymbol{x}) = \boldsymbol{\sigma}^{\infty}(\boldsymbol{x})\boldsymbol{n}(\boldsymbol{x})$ where $\sigma_{33} = p_0$ and $\sigma_{ij} = 0$ (otherwise) and, hence, $\boldsymbol{t}^{\infty} = (0, 0, p_0)$. This asymptotic condition indicates that the domain is subjected to a uniform uniaxial tension. Also, Poisson's ratio is set to be 0.25; i.e. $\lambda = \mu$. This problem is solved with the conventional BIEM, the original FM-BIEM (Fast Multipole-BIEM) and the new FM-BIEM. The numerical results obtained with the original FM-BIEM and the new FM-BIEM should be identical with those obtained with the conventional BIEM if calculations were carried out without errors caused by truncations of the infinite series. Fig.1 shows the 5736 DOF mesh and Fig.2 plots the non-dimensional crack opening displacement $\mu\phi_3/a_0p_0$ obtained with this mesh. In Fig.2 the symbols marked 'conv', 'fmm' and 'newfmm' indicate numerical results computed with the conventional BIEM, the original FM-BIEM and the new FM-BIEM, respectively. Fig.2 shows good agreement in numerical results. Fig.3 plots the total CPU time (sec) vs the number of unknowns. In Fig.3 the lines marked 'Tdir', 'Tfmm' and 'Tfmmnew' indicate the CPU time required with the conventional BIEM, the original FM-BIEM and the new FM-BIEM, respectively. This figure shows that the new FM-BIEM is only slightly faster than the original FM-BIEM. This is because this example is essentially a two-dimensional one where the computational cost for the M2L translation is not dominant. In order to show the efficiency of the new FMM more clearly we need to consider an example where boundary elements are distributed three-dimensionally. Therefore we consider many crack problems in the next example.

5.2 Many cracks

We now consider an infinite space which contains an array of penny-shaped cracks, each having the same radius a_0, subjected to the same asymptotic condition as in the previous example. The centroids of these cracks are located at the same interval of $4a_0$ in each coordinate direction, but the direction of each crack is taken random. First, we consider an array of $12 \times 12 \times 12 (= 1728)$ penny-shaped cracks (total DOF=1,285,632) in the infinite domain. Fig.4 plots the non-dimensional crack opening displacement $(\mu\boldsymbol{\phi}/a_0p_0)$ on the non-dimensional mesh $\boldsymbol{x}/a_0$. Notice that the originally flat cracks appear curved since the crack opening displacements have been superposed. The required CPU times with FM-BIEM and the new FM-BIEM are 13,954(sec) and 8,290(sec), respectively. In this example the error defined as error $= ||\widetilde{\boldsymbol{\phi}} - \boldsymbol{\phi}||/||\boldsymbol{\phi}||$ is 9.09×10^{-4}, where $\widetilde{\boldsymbol{\phi}}$ is the numerical solution obtained with the new FM-BIEM, $\boldsymbol{\phi}$ the one obtained with the original FM-BIEM and $||\cdot||$ denotes the L_2-norm. Next we consider an array of $8 \times 8 \times 8 (= 512)$ penny-shaped cracks in the infinite domain. Fig.5 plots the total CPU time (sec) required

by the original FM-BIEM and the new FM-BIEM with this array. In Fig.5 the lines marked 'Tfmm' and 'Tfmmnew' indicate the CPU times required with the original FM-BIEM and the new FM-BIEM, respectively. These results show that the new FM-BIEM is more efficient than the original FM-BIEM when the distribution of the boundary elements is more three-dimensional.

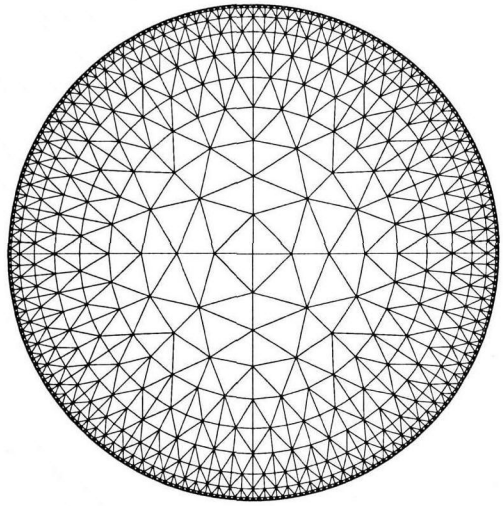

Fig. 1 crack mesh (DOF=5736)

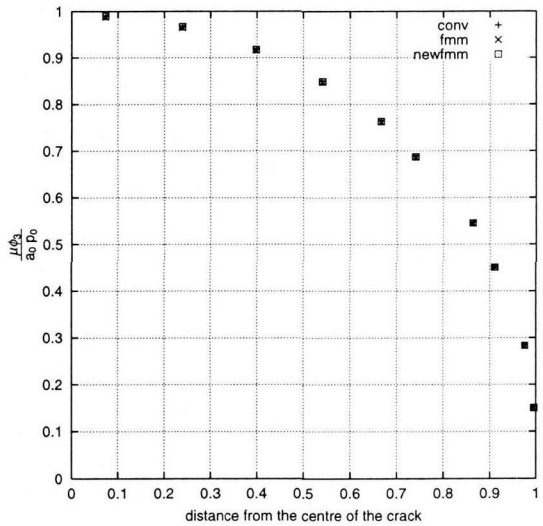

Fig. 2 crack opening displacement of one penny-shaped crack

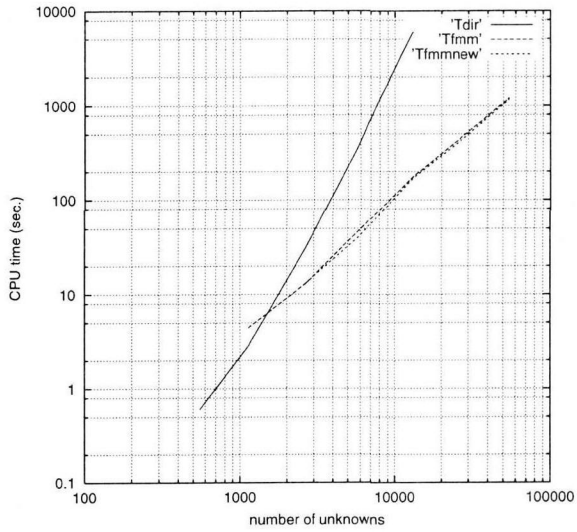

Fig. 3 CPU time (sec) for the numerical exmaples with one penny-shaped crack

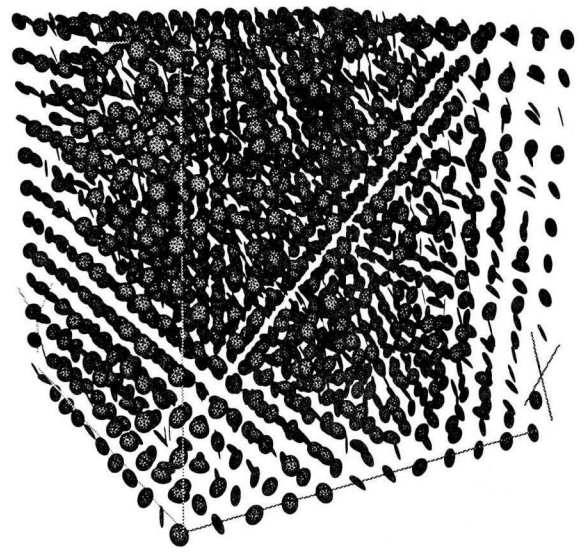

Fig. 4 crack opening displacement(DOF=1,285,632) of an array of 12×12×12 penny-shaped cracks

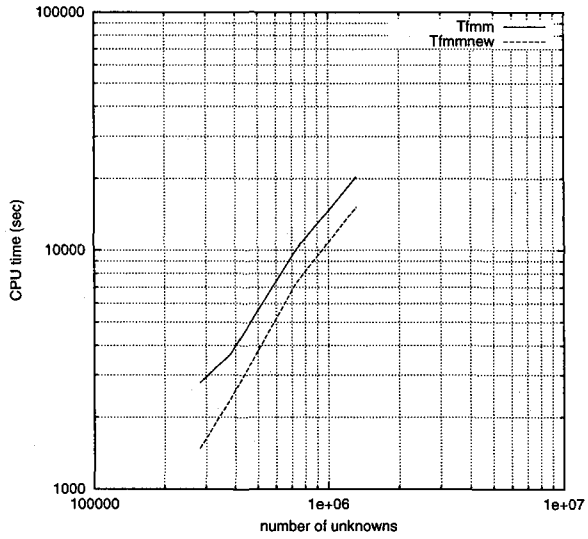

Fig. 5 CPU time (sec) for the numerical exmaples with an array of $8 \times 8 \times 8$ penny-shaped cracks

6. Conclusions

- In this paper we have succeeded in an application of the new FMM to the three-dimensional elastostatic crack problems and showed that the new FMM is faster than the original FMM in sample problems.
- We plan to use singular elements to consider the behaviour of ϕ near the crack tip and compute the stress field with FMM using techniques proposed in Yoshida et. al[8].
- The proposed techniques can be extended to the Galerkin BIEM which yields highly accurate numerical results for crack problems[8]. Also, the new FMM for the three-dimensional Helmholtz equation proposed in Greengard et al.[20] can be extended to three-dimensional elastodynamics in the frequency domain.

REFERENCES

1) Rokhlin, V.: Rapid solution of integral equations of classical potential theory, J. Comp. Phys., **60**, pp.187–207, 1985.
2) Greengard, L.: The rapid evaluation of potential fields in particle systems, The MIT Press, 1987.
3) Nishimura, N., Yoshida, K. and Kobayashi, S.: A fast multipole boundary integral equation method for crack problems in 3D, Eng. Anal. Boundary Elements, **23**, pp.97–105, 1999.
4) Fu, Y., Klimkowski, K.J., Rodin, G.J., Berger, E., Browne, J.C., Singer, J.K., van de Geijin, R.A. and Vemaganti, K.S.: A fast solution method for three-dimensional many-particle problems of linear elasticity, Int. J. Num. Meth. Eng., **42**, pp.1215–1229, 1998.
5) Fukui, T. and Kutsumi, T.: Fast multipole boundary element method in three dimensional elastostatic problems, Proc. 15th Japan Nat. Symp. BEM, **15**, pp.99–104, 1998 (in Japanese).
6) Takahashi, T., Kobayashi, S. and Nishimura, N.: Fast multipole BEM simulation of overcoring in an improved conical-end borehole strain measurement method, Mechanics and Engineering in Honor of Professor Qinghua Du's 80th Anniversary, Tsinghua University Press, pp.120–127, 1999.
7) Yoshida, K., Nishimura, N. and Kobayashi, S.: Analysis of three dimensional elastostatic crack problems with fast multipole boundary integral equation method, J. Appl. Mech. JSCE, **1**, pp.365–372, 1998 (in Japanese).
8) Yoshida, K., Nishimura, N. and Kobayashi, S.: Application of fast multipole Galerkin boundary integral equation method to elastostatic crack problems in 3D, Int. J. Numer. Meth. Engng., **50**, pp.525–547, 2001.
9) Fujiwara, H.: The fast multipole method for solving integral equations of three-dimensional topography and basin problems, Geophys. J. Int., **140**, pp.198–210, 2000.
10) Yoshida, K., Nishimura, N. and Kobayashi, S.: Analysis of three dimensional scattering of elastic waves by a crack with fast multipole bounday integral equation method, J. Appl. Mech. JSCE, **3**, pp.143–150, 2000 (in Japanese).
11) Rokhlin, V.: Rapid solution of integral equations of scattering theory in two dimensions, J. Comp. Phys., **86**, pp.414–439, 1990.
12) Rokhlin, V.: Diagonal forms of translation operator for the Helmholtz equation in three dimensions, Appl. Comp. Harmon. Anal., **1**, pp.82–93, 1993.
13) Koc, S. and Chew, W.C.: Calculation of acoustical scattering from a cluster of scatterers, J. Acoust. Soc. Am., **103**, pp.721–734, 1998.
14) Epton, M.A. and Dembart, B.: Multipole translation theory for the three-dimensional Laplace and Helmholtz equations, SIAM J. Sci. Comp., **16**, pp.865–897, 1995.
15) Elliot, W.D. and Board, J.A. JR.: Fast Fourier transform accelerated fast multipole algorithm, SIAM J. Sci. Comp., **17**, pp.398–415, 1995.
16) Dembart, B. and Yip, E.: The accuracy of fast multipole methods for Maxwell's equations, IEEE Comp. Sci. Eng., **5**, pp.48–56, 1998.
17) Hrycak, T. and Rokhlin, V.: An improved fast multipole algorithm for potential fields, SIAM J. Sci. Comp. **19**, pp.1804–1826, 1998.
18) Greengard, L. and Rokhlin, V.: A new version of the fast multipole method for the Laplace equation in three dimensions. Acta Numerica, **6**, pp.229–270, 1997.
19) Cheng, H., Greengard, L. and Rokhlin, V.: A fast

adaptive multipole algorithm in three dimensions, J. Comp. Phys., **155**, pp.468–498, 1999.
20) Greengard, L., Huang, J., Rokhlin, V. and Wandzura, S.: Accelerating fast multipole methods for the Helmholtz equation at low frequencies, IEEE Comp. Sci. Eng., **5**, pp.32–38, 1998.
21) Nishimura, N., Miyakoshi, M. and Kobayashi, S.: Application of new multipole boundary integral equation method to crack problems, Proc. BTEC–99, pp.75–78, 1999 (in Japanese).
22) Fu, Y., Overfelt, J.R. and Rodin, G.J.: Fast summation methods and integral equations: Mathematical Aspects of Boundary Element Methods (Eds. M. Bonnet, A.M. Saendig and W. Wendland), *CRC Press*, pp.128–139, 1999.
23) Yarvin, N. and Rokhlin, V.: Generalized Gaussian quadratures and singular value decomposition of integral operators, SIAM J. Sci. Comp., **20**, pp.699-718, 1998.
24) Pérez-Jordá, J.M. and Yang, W.: A concise redefinition of the solid spherical harmonics and its use in fast multipole methods, J. Chem. Phys., **104**, pp.8003–8006, 1996.
25) Biedenharn, L.C. and Louck, J.D.: Angular momentum in quantum physics: theory and application, Addison Wesley, London, 1981.
26) Nishida, T. and Hayami, K.: Application of the fast multipole method to the 3D BEM analysis of electron guns, Boundary Elements XIX, Computational Mechanics Publications, pp.613–622, 1997.

(Received September 14, 2000)